

(NASA-TN-81349) DESIGN OF A NONLINEAR
ADAPTIVE FILTER FOR SUPPRESSION OF SHUTTLE
PILOT-INDUCED OSCILLATION TENDENCIES (NASA)
31 p HC A03/AF A01 CSCL 01C

880-21355

Unclass

03/08 46843

NASA Technical Memorandum 81349

**DESIGN OF A NONLINEAR ADAPTIVE FILTER FOR SUPPRESSION OF
SHUTTLE PILOT-INDUCED OSCILLATION TENDENCIES**

John W. Smith and John W. Edwards

April 1980

NASA



NASA Technical Memorandum 81349

**DESIGN OF A NONLINEAR ADAPTIVE FILTER FOR SUPPRESSION OF
SHUTTLE PILOT-INDUCED OSCILLATION TENDENCIES**

**John W. Smith and John W. Edwards
Dryden Flight Research Center
Edwards, California**



1980

DESIGN OF A NONLINEAR ADAPTIVE FILTER FOR SUPPRESSION OF SHUTTLE PILOT-INDUCED OSCILLATION TENDENCIES

John W. Smith and John W. Edwards
Dryden Flight Research Center

INTRODUCTION

On the final flight of the space shuttle's approach and landing tests, a pilot-induced oscillation (PIO) was experienced during the flare and landing. The frequency of the PIO in the pitch axis was approximately 3.5 radians per second, and the pilot utilized a significant portion of his full control authority. Subsequent analysis confirmed the existence of PIO tendencies in this configuration, and indicated that the source of the problem was a combination of basic shuttle handling qualities, time delay through the digital flight control system computers, and rate limiting of the elevator actuators. In addition, the cockpit of the shuttle vehicle is at the approximate center of rotation of the vehicle for pitch maneuvers, which may deprive the pilot of some motion cue information.

High pilot gain during a critical task, coupled with the ability to rate limit surface actuators with large pilot inputs, is a significant factor in such PIO problems (refs. 1 to 3). Linear compensation techniques are of limited usefulness in solving this problem because of the phase lags they introduce. This report describes a PIO suppression (PICS) filter that was designed to reduce pilot gain in PIO situations with little or no phase lag. The filter is implemented as a nonlinear, adaptive element of the pilot's stick gearing schedule and operates by sensing the frequency and amplitude of the pilot's stick inputs.

The primary effect of attenuating the command path gain is to reduce the amount of rate limiting. Reducing the gain near the crossover frequency without phase lag may also result in some improvement in handling qualities, as shown in reference 4.

SYMBOLS AND ABBREVIATIONS

A, B, C, D, E, X, Y	dummy variables
ADEP	output of the smoothing filter, deg^2
AMP	amplitude
a_n	normal acceleration, g

BN	output of the control activity estimator, deg/sec
CPS	samples per second
DCGN	output of the deadband nonlinearity, deg
DEC	suppressed output of the pitch stick shaping function, deg
DEC 1	unsuppressed output of the pitch stick shaping function, deg
DEP	pilot input, deg
EDEP	ratio of filter parameters, per sec
F(s)	transfer function
K_c	forward loop gain, per sec
$K(\bar{q})$	gain constant
K_{p_θ}	pilot gain
M, N	indexes
NPTS	number of points
PILN	initial controller input equal to DEPN, deg
PIO	pilot-induced oscillation
PIOS	PIO suppression
RKP	control activity estimation equation
SKQ	output of the F-2 schedule
SQADEP	square root of the filter output along the amplitude path, deg
SQXPN	square root of the filter output along the rate path, deg/sec
s	Laplace transform variable, rad/sec
t (T)	time, sec
XPN	squared and filtered output along the rate path, deg ² /sec ²

$Y_{p\theta}(s)$	pilot model
$\dot{Z}N$	output of the control activity estimator squared, $\text{deg}^2/\text{sec}^2$
δ_e	elevator deflection, deg
θ	pitch attitude, deg
ω	frequency, rad/sec
ϕ	phase angle, deg

Subscripts:

A/C	aircraft
e	error

A dot over a quantity denotes the first derivative with respect to time.

SHUTTLE PITCH RATE COMMAND SYSTEM

A pitch rate command system is used on the space shuttle for the approach and landing phases of flight. The system is implemented as a digital flight control system resident in the shuttle's flight control computers. Figure 1 shows a conceptual block diagram descriptive of the elements important to closed-loop pitch attitude control. The pilot, designated as $Y_{p\theta}(s)$, applies a torque to a rotational hand controller which commands an output given by the following pitch stick shaping function:

$$DEC = (0.36 + 0.0484 |DCGN|) DCGN$$

The input to the stick shaping function, DCGN, results from operating on the pilot's stick position, DEP, with a $\pm 1.15^\circ$ deadband. The pitch rate command is $K_c * DEC$ in $(\text{deg/sec})/\text{deg}$; and the gain constant for the approach and landing, K_c , remains constant at a value of 0.4. Pitch rate control is achieved by positive feedback around the power actuator and servo, yielding an equivalent system for the actuator loop, with a "free s" in the denominator. As such, the error signal, which is made up of the commanded response and aircraft pitch rate, is continually driven to zero. The integration rate is proportional to the scheduled gain due to dynamic pressure, $K(q)$, and is approximately equal to 1.446. The remaining terms left in the closed-loop transfer functions are:

$$F(s) = 1.395 \frac{(s/1.5 + 1)(s/1.8 + 1)}{(s/21.5 + 1)(s/2.7 + 1)}$$

Inside the actuator and servo loop, the rate at which the actuator can move is restricted to ± 20 deg/sec. The filters, gains, summations, rate restrictions, and pitch stick shaping function are implemented in the shuttle's digital flight control computers.

PILOT-INDUCED OSCILLATION SUPPRESSION FILTER

Description and Design Logic

In general, the objectives of the PIOS filter are simple: to modify the stick shaping function, $DEC = f(DCGN)$, as a function of the frequency and amplitude of the pilot's input to acquire the desired gain reduction; and, at the same time, to minimize phase lags introduced by the filter.

The filter developed to achieve these objectives is diagramed in figure 2. The blocks of the diagram present all the elements, mathematical computations, and logic of the filter in a sequential manner. The dynamic elements, shown as Laplace transformed functions, are implemented as digital filters. The FORTRAN program used to implement the filter is listed in appendix A.

The PIOS filter contains a frequency- and amplitude-sensitive element composed of a second-order lag-lead filter

$\left(\frac{1}{4} \frac{(s + 20)^2}{(s + 10)^2} \right)$; two rectifiers; two first-order filter smoothers; and a modifying function, SKQ, for the quadratic term of the stick shaping function. The PIOS filter operates by obtaining an estimate, EDEP, of the dominant frequency of the pilot's input. This estimate is used to modify the quadratic term of the stick shaping function in order to preclude the possibility of rate limiting the control surface actuators.

The pilot's input, DEP, is displaced by the deadband ($\pm 1.15^\circ$) and then goes to both the pitch stick shaping function and the elements of the PIOS filter. The pitch stick shaping function implemented on the shuttle (fig. 3) is given by

$$DEC_1 = (0.36 + 0.0484 |DCGN|) DCGN$$

The combination of linear and quadratic terms in the gearing is intended to give acceptable handling qualities for small inputs while also allowing full control surface authority.

The output of the summation junction in the PIOS filter paths, BN (fig. 2 and below), essentially serves as a control activity estimator. It is defined as follows:

$$BN = \left[1 - \frac{1}{4} \frac{(s + 20)^2}{(s + 10)^2} \right] DCGN$$

$$= \left[\frac{3s(s + 13.33)}{4(s + 10)^2} \right] DCGN$$

This quantity, BN, then is rectified (X^2) and smoothed by a low pass filter. The square root of the resulting quantity, SQXPN, is proportional to the frequency and amplitude of the low frequency components of the pilot's input. The same mathematical operations are carried out along the amplitude-estimating path, providing a quantity proportional to the amplitude of the pilot's input. The F-1 schedule (fig. 4(a)) serves two purposes. First and foremost, the schedule is necessary to avoid subsequent division by zero. However, to lessen the suppressed response for step inputs of 5° and less, the minimum value is limited to 4.5° . A ratio of the two paths is obtained to eliminate the amplitude effect, making EDEP primarily proportional to the frequency of the control activity. The F-2 schedule (fig. 4(b)) controls the amount of suppression provided by the filter. The minimum value of the F-2 schedule (-0.15) limits the maximum suppression of the filter. The design philosophy regarding the time constants and schedules for this particular example is given in appendix B.

Digital Computations and Simulations

Figure 5 presents the results of a digital simulation using the FORTRAN listing given in appendix A. Pertinent filter elements are shown as a function of time when forced by a sinusoidal pilot input, DEP. The peak input amplitude is 10° at a frequency of 3 radians per second for 3.25 cycles. The "notching" of BN and ZN is due to the deadband. However, this effect is smoothed out by the first-order filter. Parameters downstream of the first-order smoothing filters illustrate the 3.3 second settling time. In particular, the SKQ trace is approaching its minimum value of -0.15 . For this set of conditions, the F-2 schedule was designed to almost limit the maximum amount of suppression and the final value of the stick shaping function, DEC. DEC is reduced to about 43 percent of the unsuppressed output, DEC 1, and this value is almost reached after three cycles. The steady-state suppression and settling time for this example were chosen as the design objectives (appendix B).

Cross plots of the output-to-input relationships for input amplitudes of 17° , 10° , and 5° are presented in figure 6. The sinusoidal input frequency is 3 radians per second and oscillates for five complete cycles.

For the 17° input (fig. 6(a)) the final suppressed output is approximately 5° , and was nearly reached after two cycles. This particular characteristic of the PIOS filter is due to the time constant of the first-order filter and the F-2 schedule. The final suppressed output is about 28 percent of the unsuppressed output shown in figure 3. There is very little hysteresis, even at the extreme input, and none at 0° of DEP. Figure 6(b) presents the cross plot for a 10° input. The same general trends as for the 17° input amplitude response are evident. The final suppressed output for a 10° input is 3° , which is about 43 percent of the unsuppressed output. Figure 6(c) shows a cross plot of the output-to-input ratio for 5° of input amplitude. Very little suppression is evident. The final output is about 75 percent of the unsuppressed value. This characteristic is due primarily to the minimum value (4.5) set on schedule F-1.

Information similar to that presented in figure 6 can be summarized over the frequency range of interest. Figure 7 presents the final suppressed output of the PIOS filter for three different input amplitudes (17° , 10° , and 5°) over a frequency range from 0 to 7 radians per second. Two characteristics are apparent. First, at frequencies above 4 radians per second the suppressed output is constant for all conditions. This is because the minimum value in schedule F-2 (-0.15) has been reached. Second, at frequencies below 3 radians per second, the reduction in output is almost linear with frequency. Finally, at low input frequencies, there is very little suppression for an input amplitude of 5° .

Figure 8 presents the time response of the pilot command with and without the PIOS filter for a 5° and 10° step input. The trace for the 5° step input shows the effects of the design consideration placed on the F-1 schedule in that SQADEP had a minimum value of 4.5 (fig. 4(a)). The output of the PIOS filter, DEC, for a 5° step is within 85 percent of the unsuppressed value. For a 10° step input, the output of the shaping function varies from a minimum value of 3.7° at 0.25 second to almost 6° at 4 seconds. The rise rate of the output response, DEC, is governed by the time constant (3.3 sec) in the first-order smoothing filter. This time-dependent response would reduce the amount of surface rate limiting due to large step inputs.

Open-Loop Response

The actual pilot input, DEP, during the shuttle landing when the PIO occurred was used as the input to the filter to illustrate the PIOS filter's behavior. Even though this simulated approach is strictly open loop, the output of the PIOS filter is indicative of the control surface motion to be expected under similar circumstances with the PIOS filter in operation. Figure 9 presents the response of pertinent PIOS filter parameters due to the pilot input, DEP, as generated from the data recorded during the flight. During the approach from 0 to approximately 20 seconds, the amount of suppression varies, as is evident in the governing parameter SKQ. For this time span, SKQ is always less than 1.0 and averages about 0.5. During the PIO, between 25 and 35 seconds, the peak inputs were

about $\pm 10^\circ$ at a frequency of between 3 and 4 radians per second. The SKQ parameter for this period of time would have reached a minimum value at about 25 seconds. This would have occurred just prior to landing and throughout the landing phase. The suppressed output, DEC, compared with the unsuppressed output, DEC 1, is noticeably less throughout the latter part of the flare and landing maneuver. For this example and with respect to the predicted rate limiting, the PIOS filter is designed to offer the desired amount of suppression following the logic developed in appendix B.

Closed-Loop Analysis

Observation of the actual closed-loop behavior of the PIOS filter would undoubtedly permit a more meaningful assessment of its worth. Therefore, a constant gain pilot model K_{p_θ} (fig. 1) was mechanized on a simulator of the shuttle flight dynamics. Simulator (fig. 1) responses were obtained with and without the PIOS filter included. Figure 10(a) shows the characteristics of the simulated shuttlecraft with pitch attitude feedback and basic stick shaping for a pilot gain, K_{p_θ} , of 7.2. This gain was selected for this example as the gain where instability would begin to occur. With the PIOS filter (fig. 10(b)), the system was stable, with a subsidence ratio of -0.38, and would have taken about one cycle to damp out. Both systems were pulsed with a pitch input of 1° .

Figures 11(a) and 11(b) present the variation of subsidence ratio and frequency, respectively, with gain. At a pilot gain of 4, both systems are well damped. With the PIOS filter, about twice the gain margin is realized, and for higher gains the oscillations are bounded. The oscillation frequency approaches 3.0 radians per second. The damped frequency is the same for low pilot gain and somewhat less with the PIOS filter below the divergent gain.

CONCLUSIONS

A nonlinear adaptive filter was designed to suppress the pilot-induced oscillations (PIO) tendencies of the space shuttle vehicle. From digital computations and simulations, it can be concluded that:

(1) The PIOS filter attenuates the gain of the pitch stick shaping function without adding phase lag to the system.

(2) With the pitch attitude loop on a shuttle simulator model closed, the PIOS filter demonstrated a gain margin increase by a factor of about two.

*Dryden Flight Research Center
National Aeronautics and Space Administration
Edwards, California, March 5, 1980*

APPENDIX A - COMPUTER PROGRAM FOR PILOT-INDUCED OSCILLATION SUPPRESSION WITH SINE WAVE INPUT

```

PROGRAM SFILTER (INPUT,OUTPUT,TAPE1=INPUT,TAPE2)

NAMELIST /FILNAM/ AMP,OMEGA,CPS

C ***** SET INITIAL AND CONSTANT VALUES.
CALL PLTTS (0,7,3)
CALL FACTOR (0.3937)
1 READ (1,160)
100 FORMAT (A10)
IF (LCF(1).NE.0) GO TO 999
BACKSPACE 1
READ FILNAM
PRINT 101, AMP,OMEGA,CPS
101 FORMAT (1H1,"AMP = ",F4.1,"X","OMEGA = ",F3.1,"X","CPS = ",F5.1,/)
PRINT 102
102 FORMAT (1H1,"TIME",9X,"DEPN",9X,"BN",9X,"ZN",9X,"XPN",9X,"SOXPN",
  2 9X,"SQADFP",9X,"EDFP",9X,"SKO",9X,"DEC1",9X,"DEC",/)
T = 1.0/CPS
NPTS = 5.000628320CPS/OMEGA+0.5
A = -2.0*EXP(-20.0*T)
B = EXP(-40.0*T)
C = -2.0*EXP(-10.0*T)
D = EXP(-20.0*T)
E = EXP(-30.0*T)
F = 0.5*(1.-F)
RKP = ((1.0-EXP(-10.0*T))**2)/((1.0-EXP(-20.0*T))**2)
YNM1 = YNM2 = DEPNM1 = DEPNM2 = XPNM1 = ZNM1 = 0.0
ADEPN=A*DEPN1+DEPN2=DEPN21=0.
C ***** LOOP TO COMPUTE DEP AND DEC FOR 5 CYCLES.
N = -1
DO 1 N = 1
IF (N.GT.NPTS) GO TO 4
FILN = AMP * SIN(N*OMEGA*T)
DEPN = FILN
IF (ABS(DEPN).LE. 1.15) DCGN = 0.0
IF ((DEPN).GT. 1.15) DCGN = DEPN-1.15
IF ((DEPN).LT. -1.15) DCGN = DEPN +1.15
DEPN = DCGN
YN = (-YNM1)-D*YNM2+RKP*(DEPN+A*DEPNM1+B*DEPNM2)
BN = (DEPN-YN)
ZN = (BN)**2
XPN = XPNM1+F*(ZN+ZNM1)
SOXPN = SQRT(XPN)
DEPN = C*DEPN+DEPN
ADEPN = A*ADEPN1+F*(DEPN-DEPN21)
SQADFP = (SQRT(ADEPN))
IF (SQADFP.LT.4.5) SQADFP = 4.5
EDFP = SOXPN/SQADFP
SKO = 1.-(1./EDFP)
IF (SKO.LT.-.15) SKO = -.15
DEC1 = DCGN*(.36+0.04*ABS(DCGN))
DEC = DCGN*(.36+SKO*.04*ABS(DCGN))
IF (NPTS.GT.1) AND (PCD(N,10).NE.0) GO TO 3
IF (NPTS.GT.1) AND (MOD(N,17).NE.0) GO TO 3
TIME = N
PRINT 103,11H,FILN,BN,ZN,XPN,SOXPN,SQADFP,EDFP,SKO,DEC1,DEC
103 FORMAT (1X,11(1F10.5,2X))
WRITE (2) FILN,DFC
YNM2 = YNM1
YNM1 = YN
DEPNM2 = DEPNM1
DEPNM1 = DEPN
XPNM1 = XPN
ZNM1 = ZN
ADEPN1 = ADEPN
DEPN21 = DEPN2
GO TO 2
4 PRINT
C ***** CALL SUBROUTINES TO DO TIME HISTORY AND CROSS PLOTS.
CALL THIST (AMP,OMEGA,CPS)
CALL CPLET (AMP,OMEGA,CPS)
GO TO 1
999 CALL PLT (1,0,0,0,0)
END

```

APPENDIX B - CONSIDERATIONS IN PILOT-INDUCED OSCILLATION SUPPRESSION FILTER DESIGN

During the final flight of the shuttle approach and landing tests, during the period when the pilot was experiencing a PIO, control inputs were being made at a rate of 3 to 4 radians per second at peak amplitudes of $\pm 10^\circ$ of rotational hand controller travel. Since the inputs were sufficient to rate saturate the elevator, this experience was an excellent example of the type of encounter a suppression filter should be designed to prevent.

Figure 12 presents the rate saturation boundaries, the maximum surface travel limits, and the linear response of the elevator for 10° of controller travel, all as a function of frequency. The circle symbols represent nonlinear calculations of the actual rate limit response. The solid line indicates the total rate limiting that would occur in a sawtooth fashion. The dashed line represents the frequency and amplitude where barely perceptible rate limiting would occur. The PIO frequency, as pointed out, is between 3 and 4 radians per second. For example, if the PIOS filter is to avoid perceptible rate limiting, the forward loop gain would have to be reduced to approximately 38 percent of the linear value at 4 radians per second.

Since the frequency is less than 10 radians per second, a rate sensing element of $1 - \frac{1}{4} \frac{(s + 20)^2}{(s + 10)^2}$ was selected. This expression can be simplified to $\frac{3}{4} \frac{s(s + 13.33)}{(s + 10)^2}$. Figure 13 presents the frequency response of this rate-sensing function and illustrates the differentiation at low frequencies caused by the "free s" of the latter expression. As indicated, the gain is fairly linear with frequency from 0 to 4 radians per second. Therefore, this function would be a reasonable estimator of frequency. The output of the rate-sensing function plus the control input is squared (fig. 2), then filtered with a first-order lag with a 3.3 second time constant. The smoothed output of the filter is then reverted back as the square root. The ratio of the two time-dependent parameters, $\frac{SQXPN}{SQADEP}$, may thus be used as an estimate of the input frequency, EDEP. The F-1 schedule (fig. 4) avoids division by zero and is further removed than necessary to give an unsuppressed step response for small controller inputs (inputs less than 4.5°). The F-2 schedule (fig. 5) is used to limit the maximum amount of suppression. Selecting this value causes the output of EDEP to be determined as a function of frequency and amplitude (fig. 14). For a sinusoidal input, with a peak amplitude of 10° at the PIO frequency, the final value of EDEP would be approximately 0.3. In order to reduce the forward loop gain to 0.38 at 10° of controller input, the output of the pitch stick

shaping function would have to be reduced from 6.98° to 2.62° . This will make the desired minimum value for SKQ equal to -0.15. The schedule then is designed to intersect the minimum value of EDEP at 0.3, as shown in figure 4(b).

REFERENCES

1. Ashkenas, Irving L.; Jex, Henry R.; and McRuer, Duane T.: Pilot-Induced Oscillations: Their Cause and Analysis. TR-239-2, Systems Technology, Inc., June 20, 1964.
2. Smith, John W.; and Berry, Donald T.: Analysis of Longitudinal Pilot-Induced Oscillations Tendencies of YF-12 Aircraft. NASA TN D-7900, 1975.
3. Smith, John W.: Analysis of a Lateral Pilot-Induced Oscillation Experienced on the First Flight of the YF-16 Aircraft. NASA TM X-72867, 1979.
4. Smith, Ralph H. . Evaluation of Space Shuttle Orbiter Longitudinal Handling Qualities in Approach and Landing. Systems Research Lab., Inc. (2800 Indian Ripple Rd., Dayton, OH 45440), Aug. 1979.

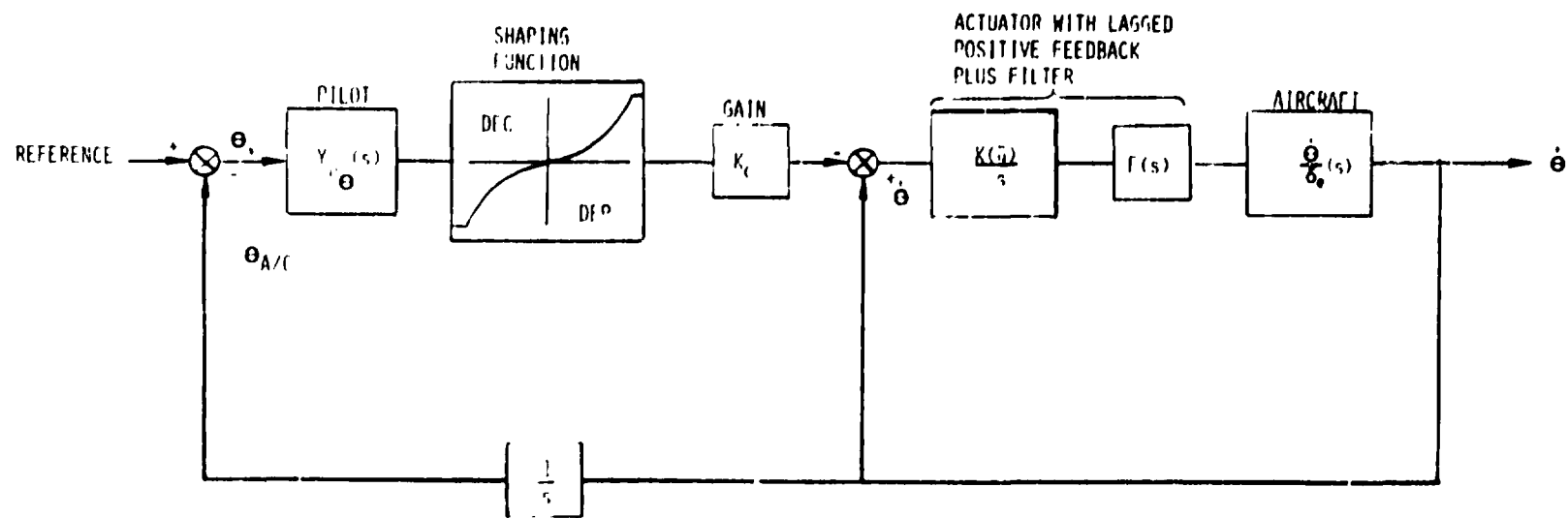


Figure 1. Conceptual block diagram of the shuttle control system with the pilot closing the pitch attitude loop.

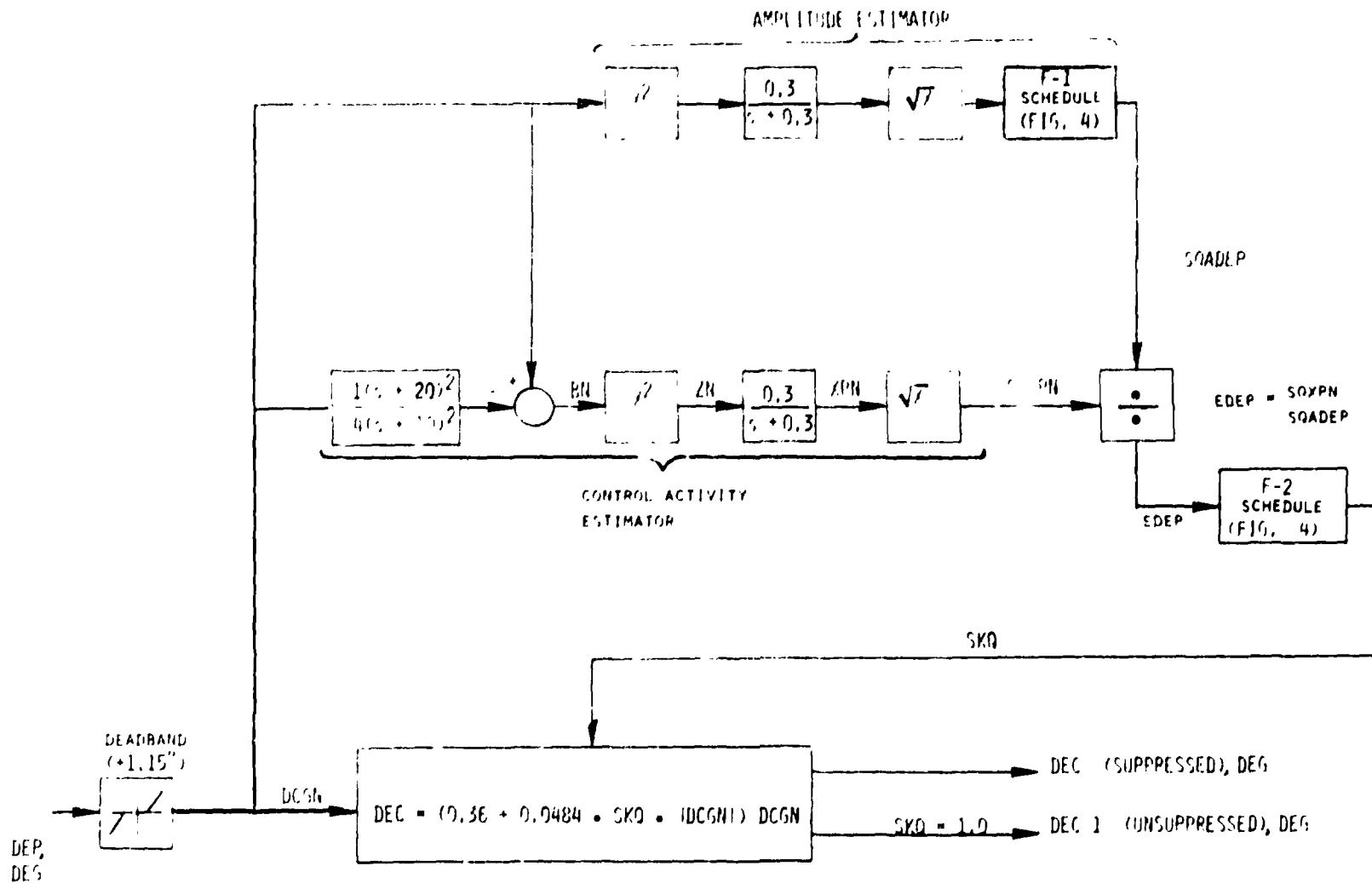


Figure 2. PIOS filter logic and shuttle pitch stick shaping function.

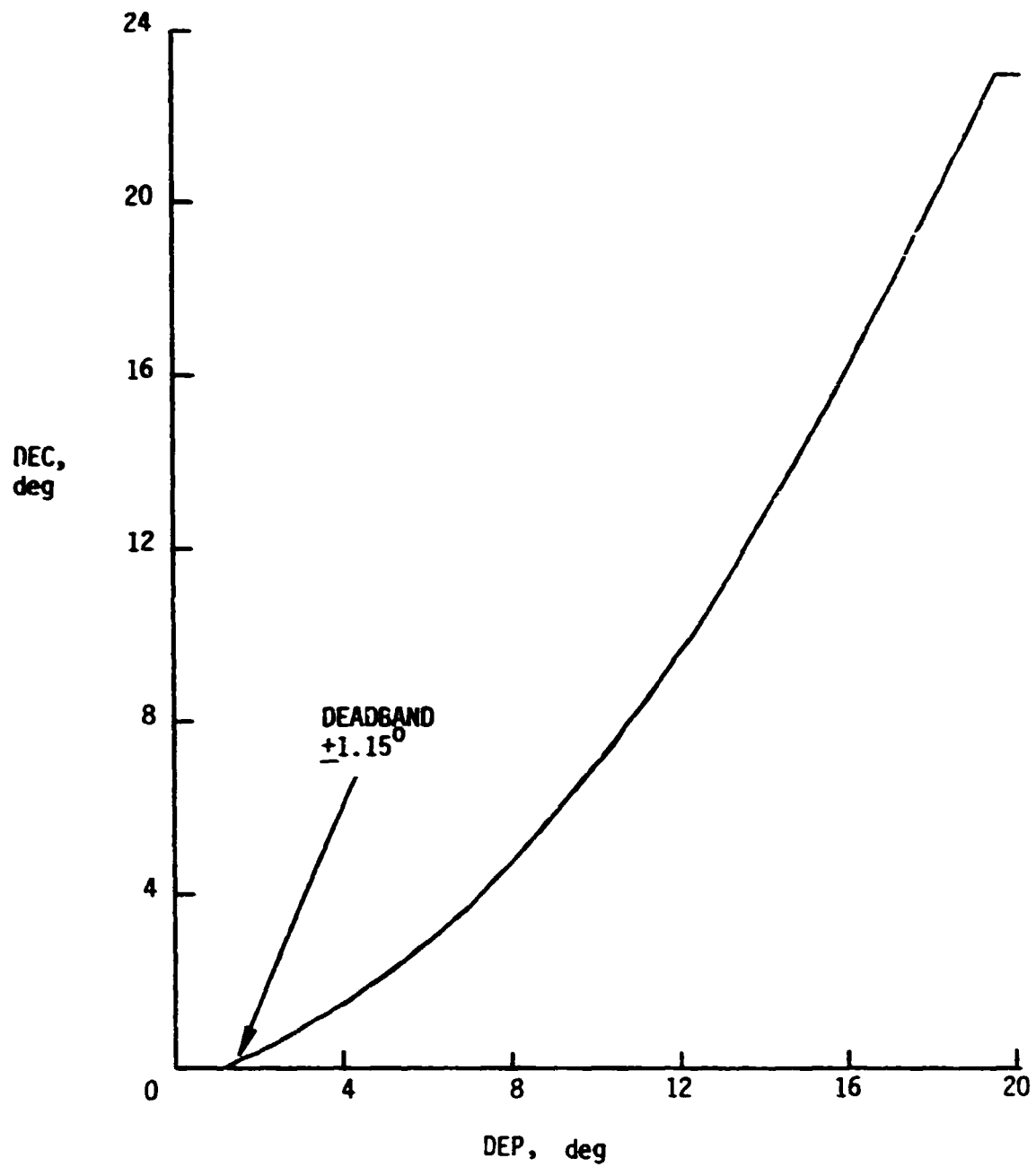
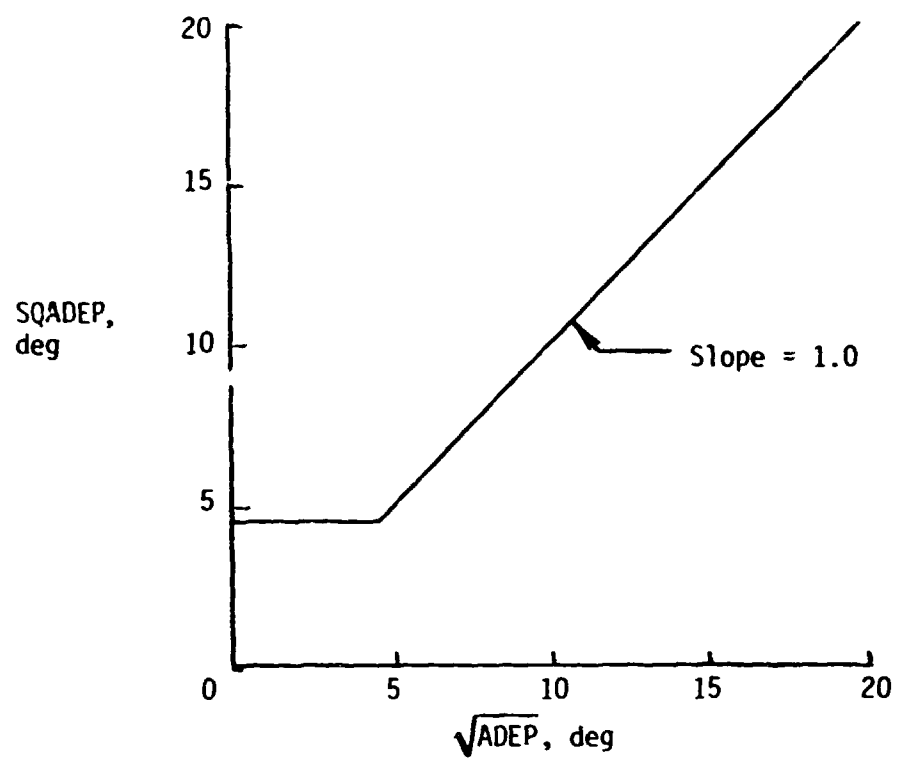
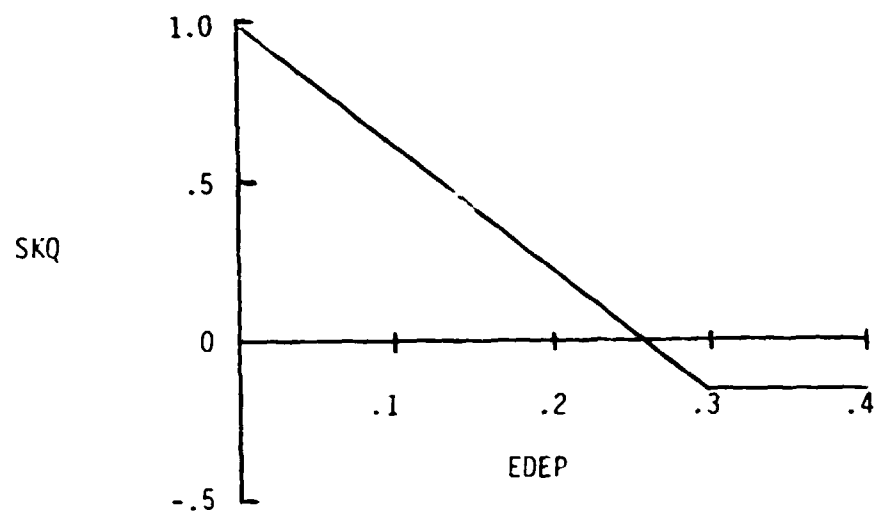


Figure 3. Shuttle pitch stick shaping when SKQ equals 1.0 (fig. 2). DEC equals $(0.36 + 0.0484 \cdot SKQ \cdot |DCGN|) \cdot DCGN$ where DCGN includes the deadband.



(a) F-1 schedule. If SQADEP is less than 4.5, SQADEP equals 4.5.



(b) F-2 schedule. If SKQ is less than -0.15, then SKQ equals -0.15.

Figure 4. PIOS filter schedules (fig. 2).

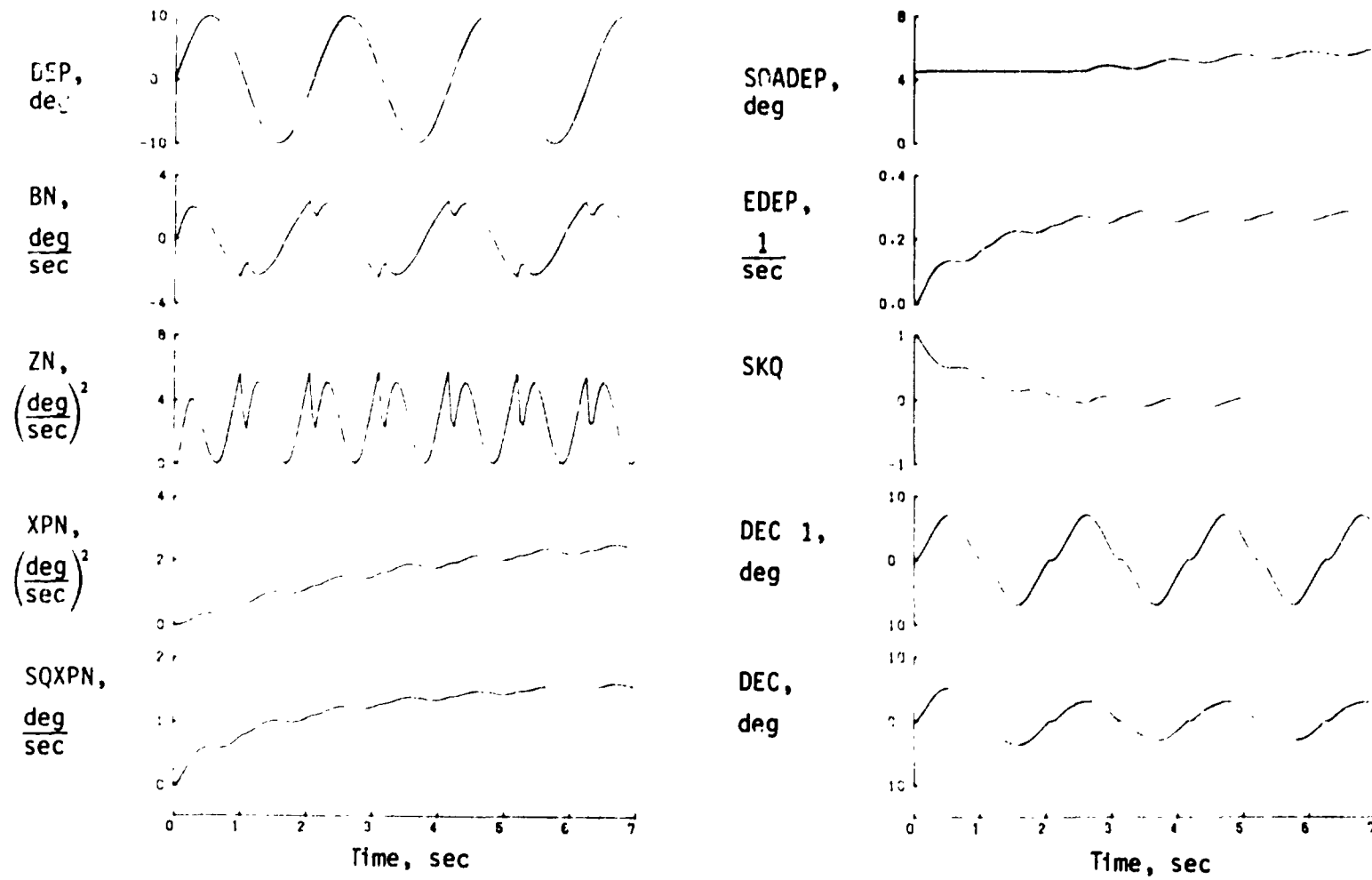
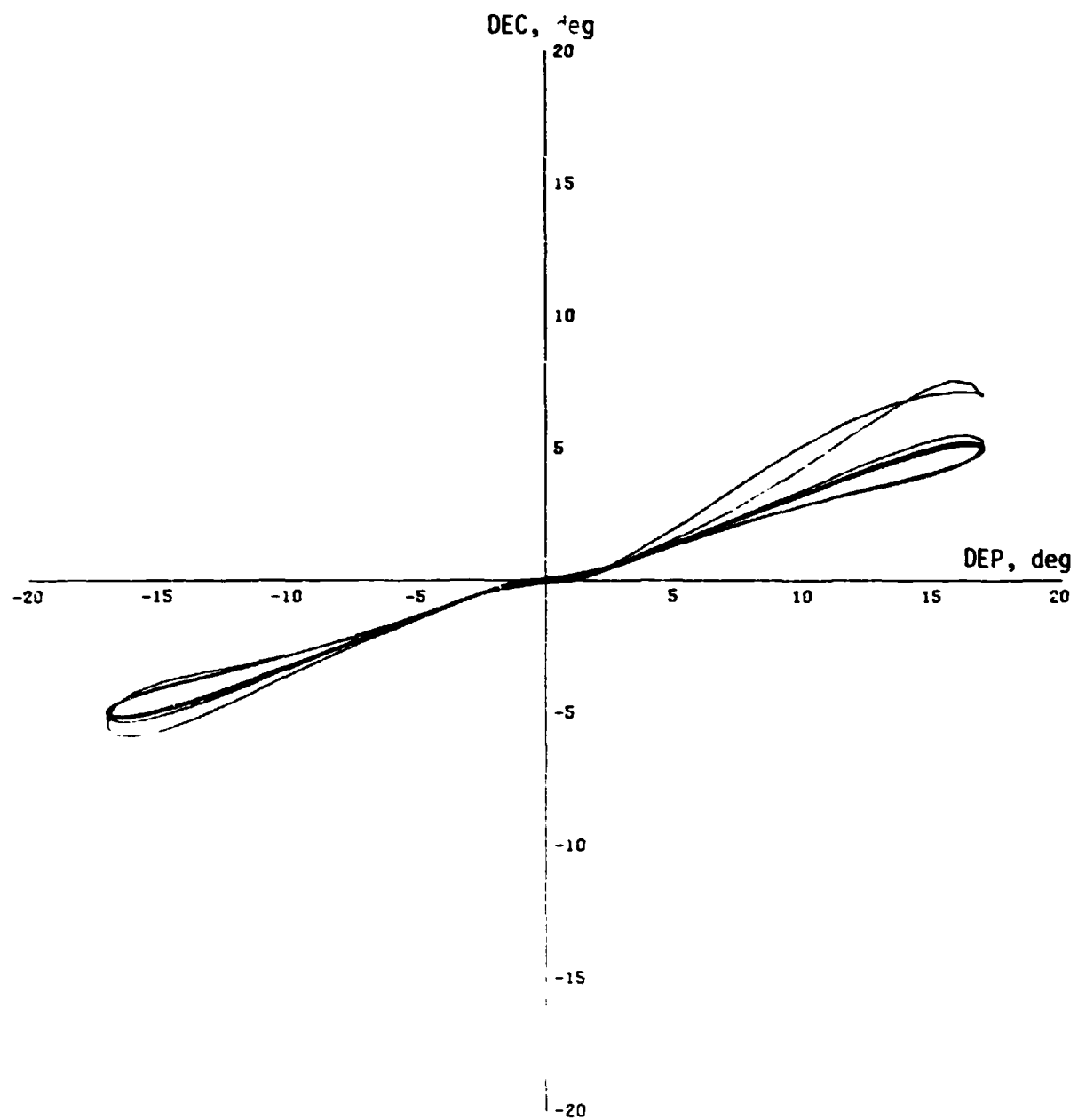
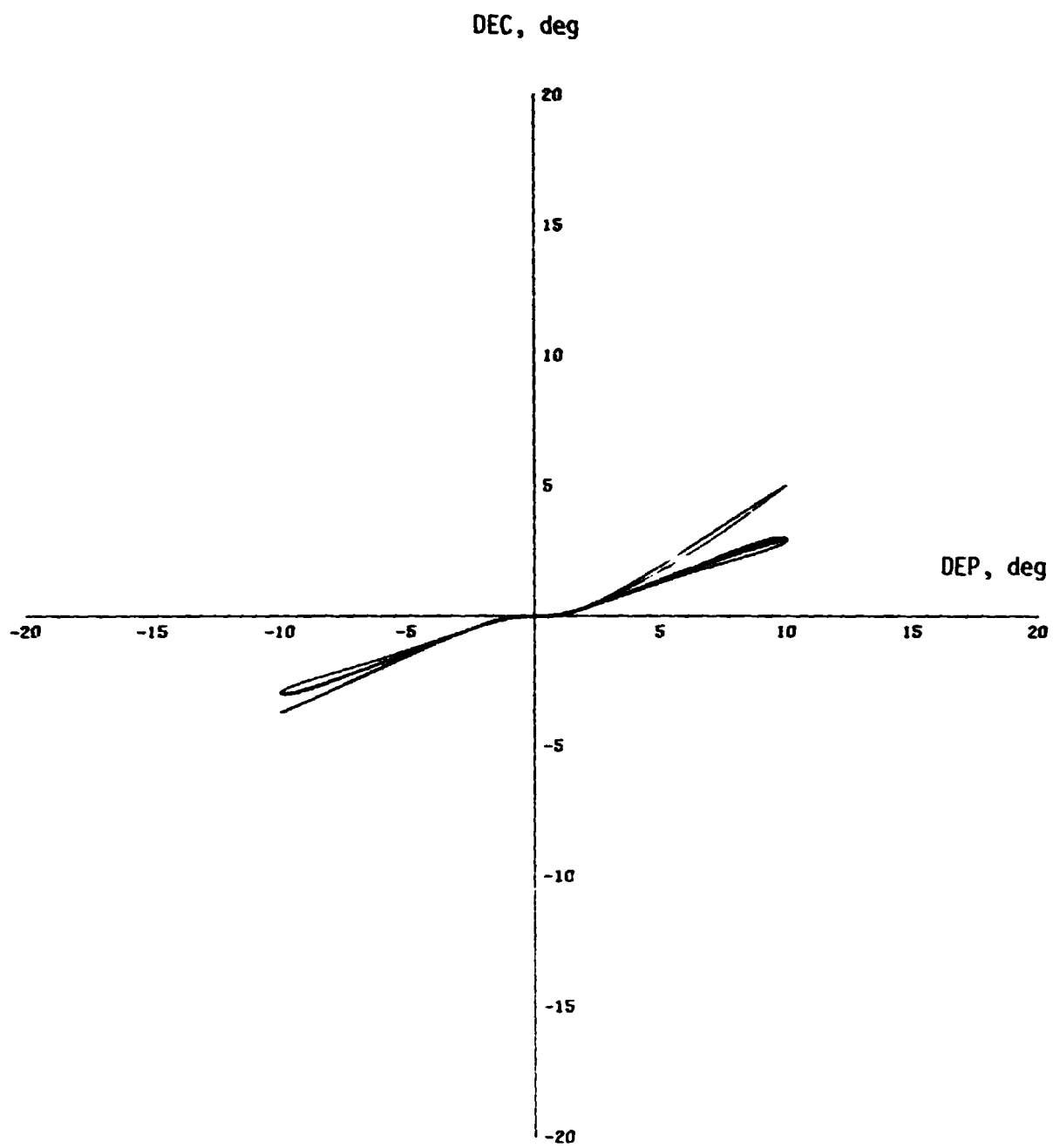


Figure 5. Output of the PIOS filter parameters with time for a sine wave input. $\text{DEP} = 10^0 \sin \omega t$ ($\omega = 3 \text{ rad/sec}$).



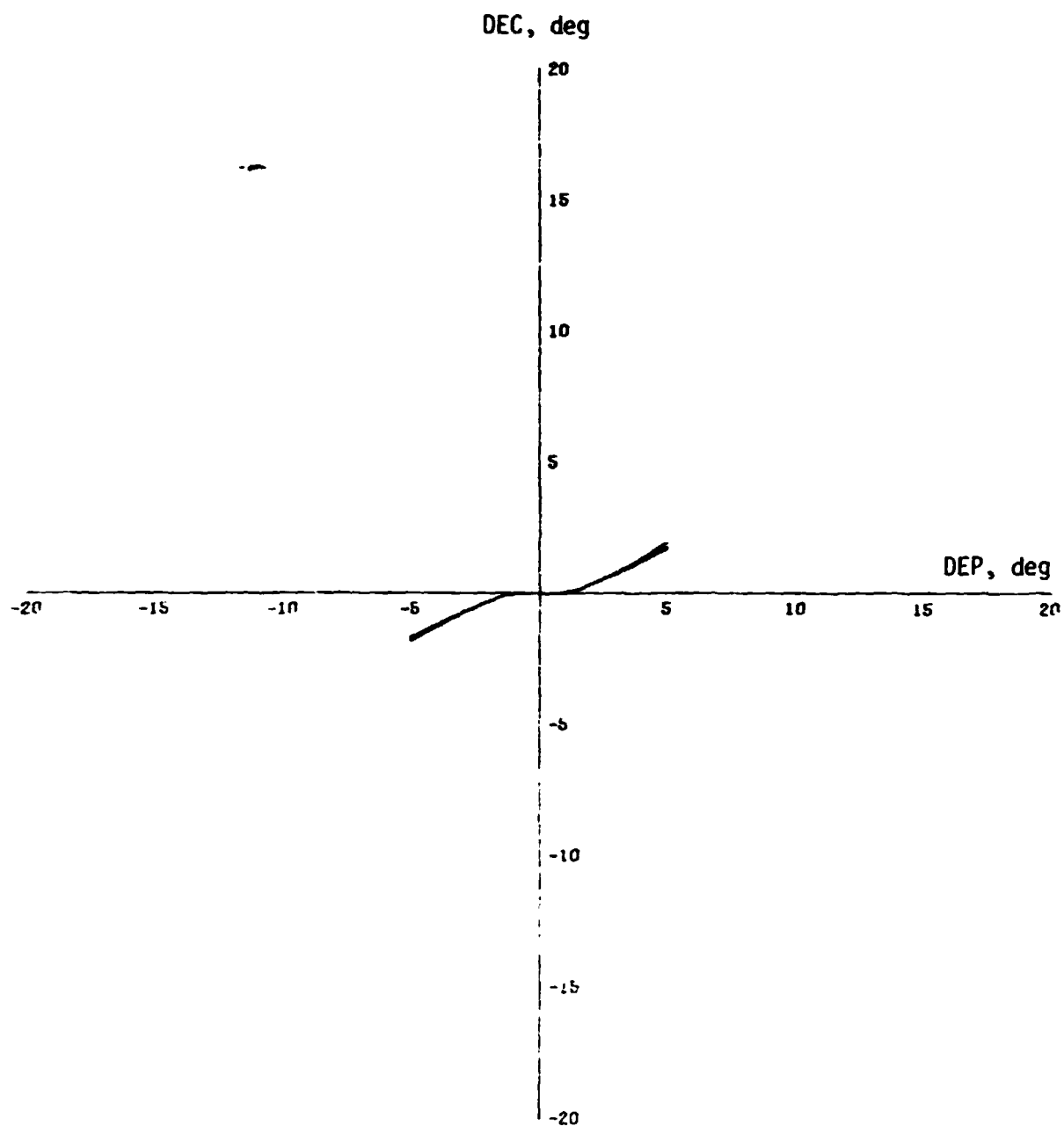
(a) $DEP = 17^{\circ} \sin \omega t$.

Figure 6. Cross plot of the PIOS filter characteristics through five complete sine wave cycles at a frequency of 3 rad/sec.



(b) $\text{DEP} = 10^0 \sin \omega t$.

Figure 6. Continued.



(c) $DEP \approx 5^\circ \sin \omega t$.

Figure 6. Concluded.

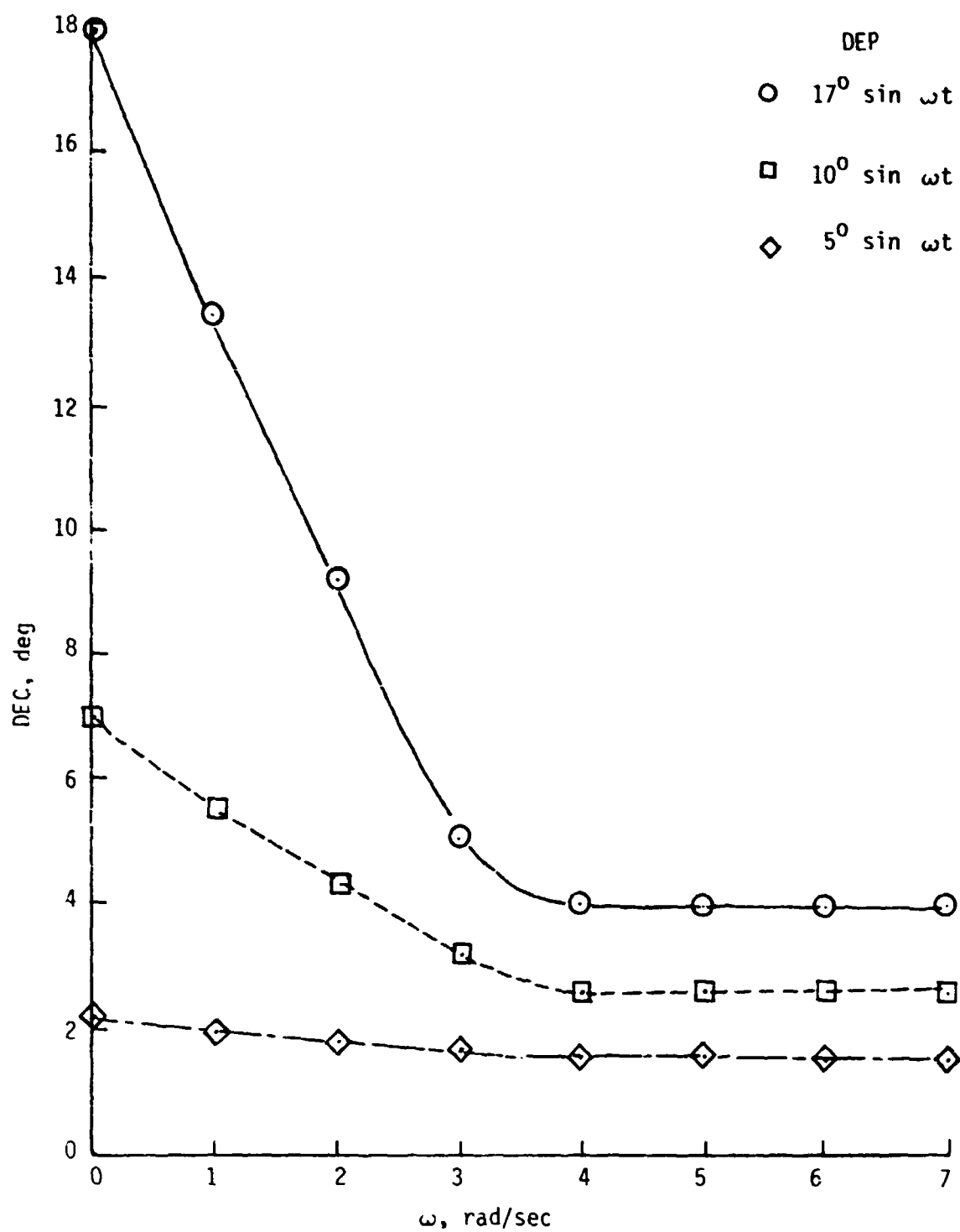
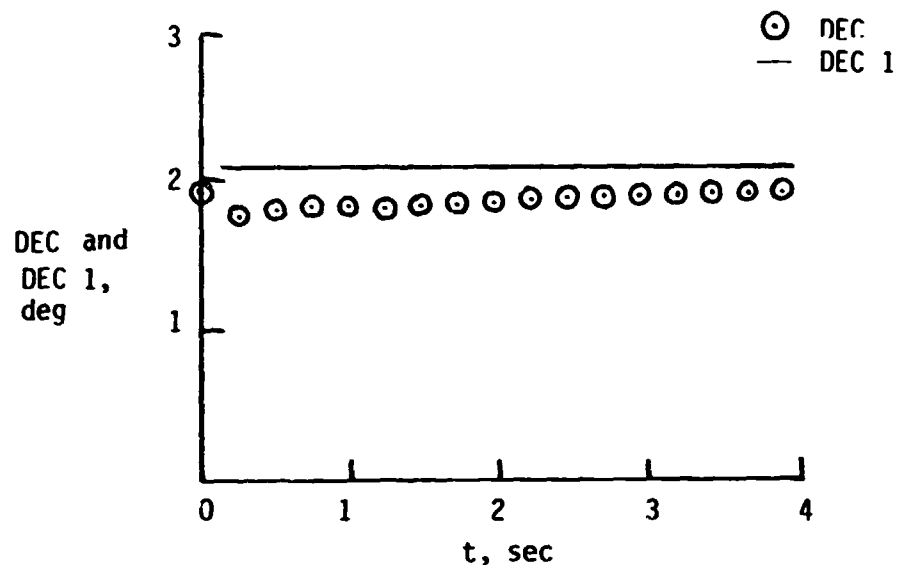
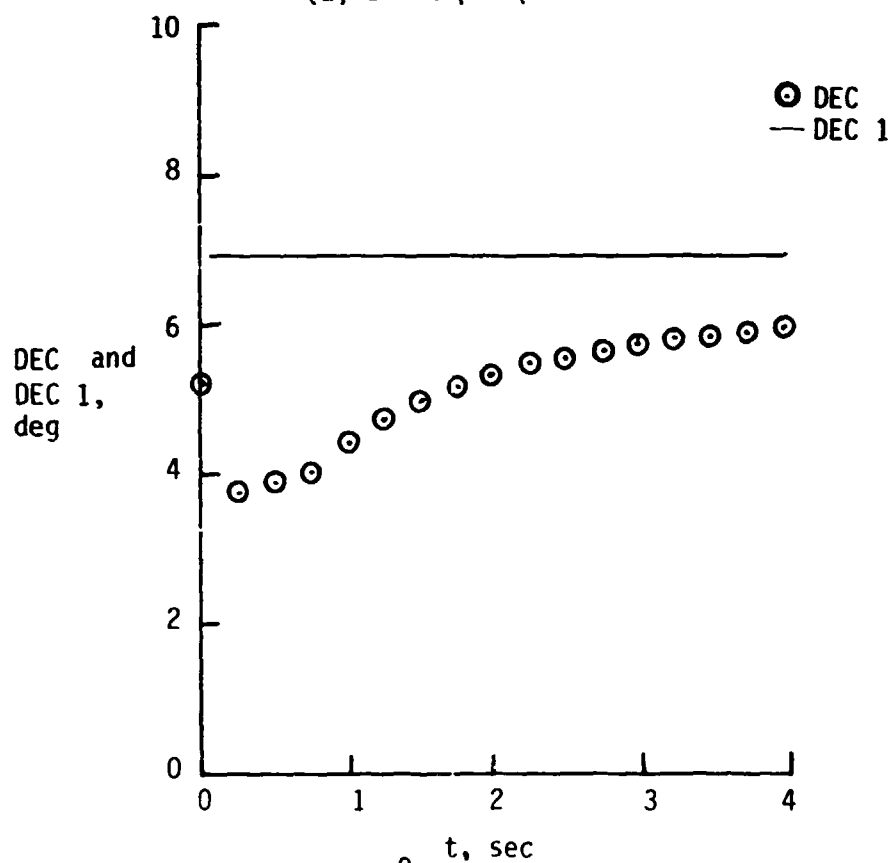


Figure 7. Final suppressed output of the pitch stick shaping logic with the PIOS filter implemented.



(a) 5° step input to DEP.



(b) 10° step input to DEP.

Figure 6. Output to a step response in the pitch stick shaping logic with and without the PIOS filter.

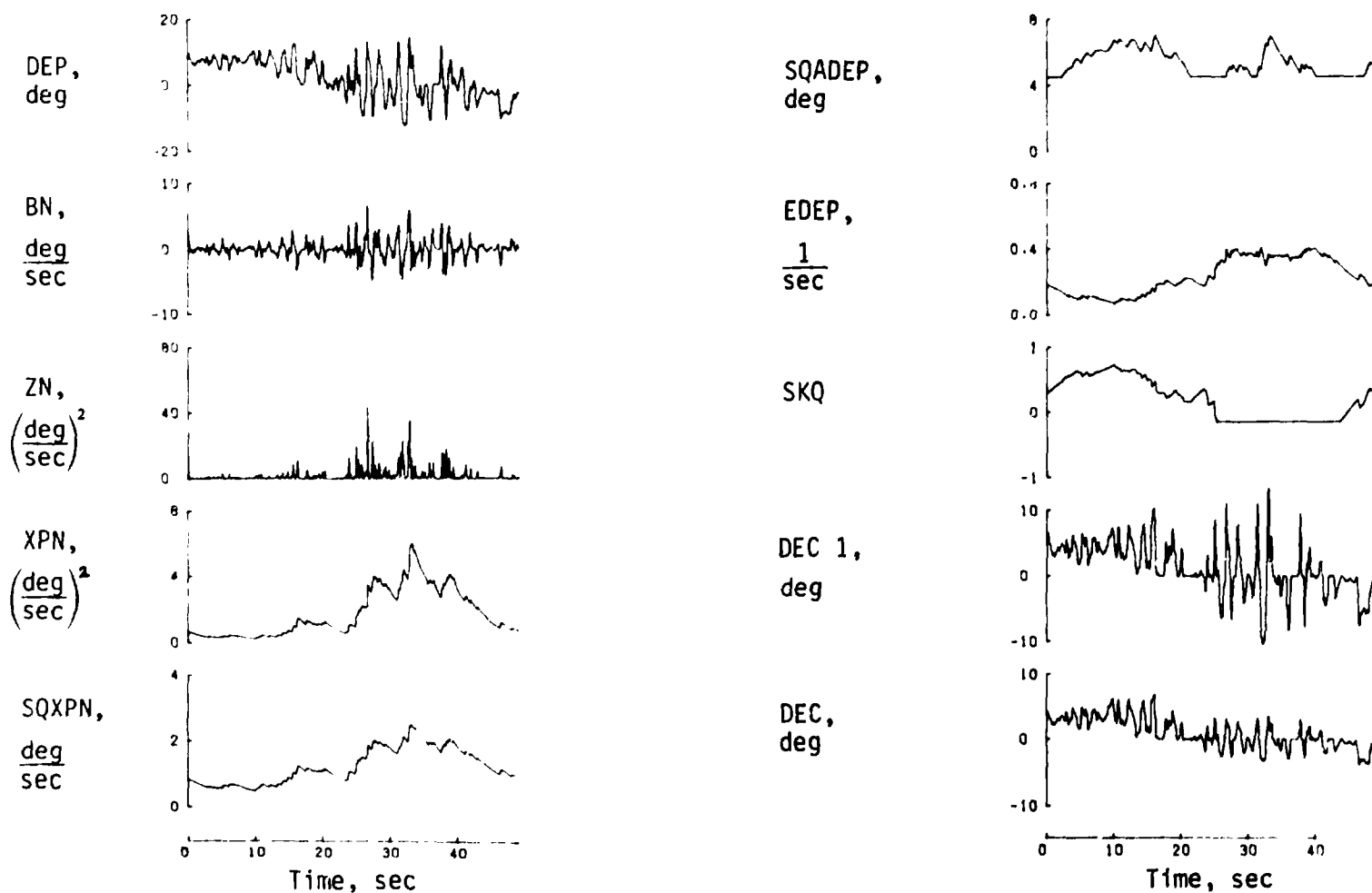


Figure 9. Open-loop response of PIOS filter parameters with time. The pilot input data, DEP, were taken from a shuttle approach and landing during which a PIO occurred.

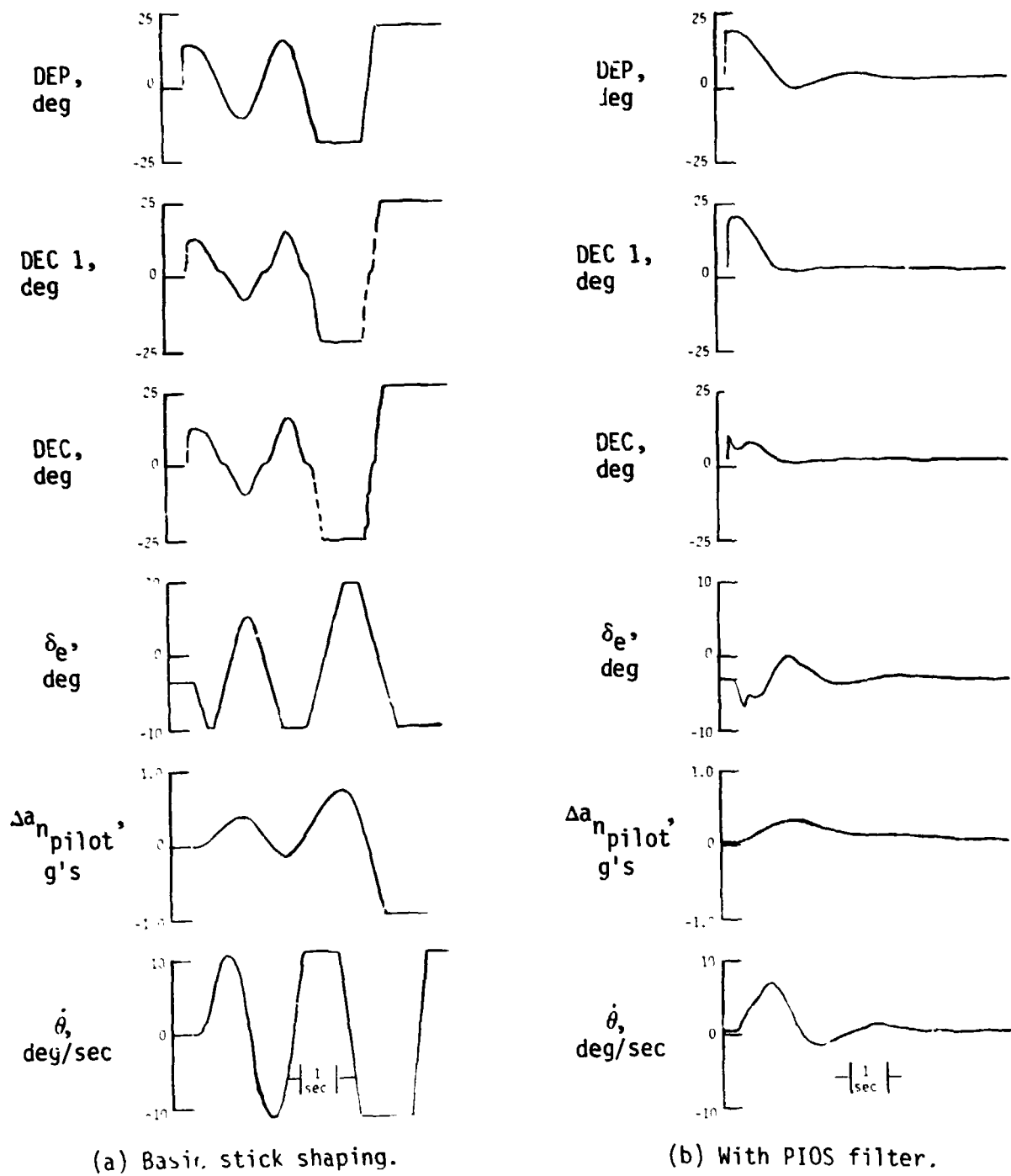
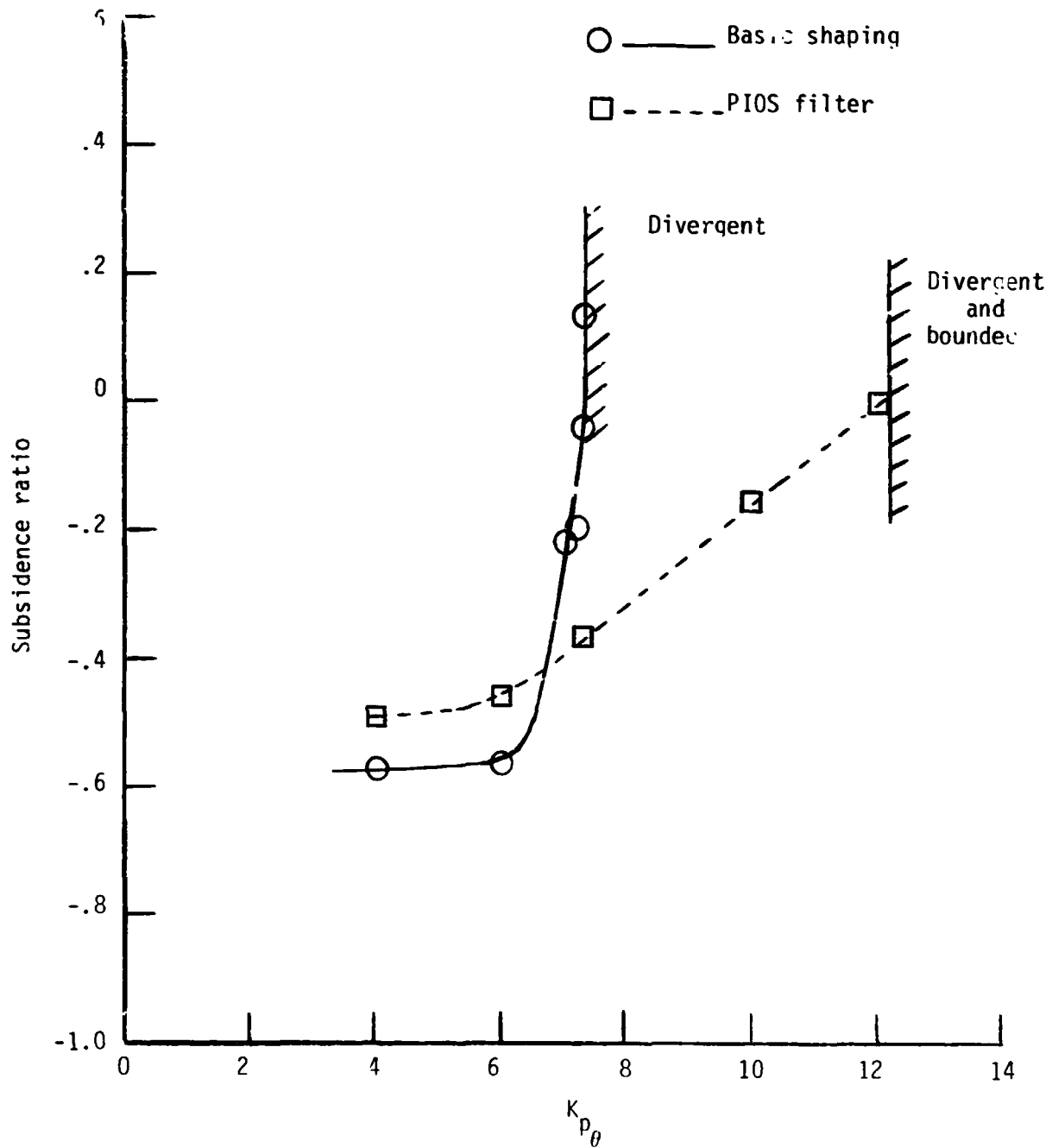
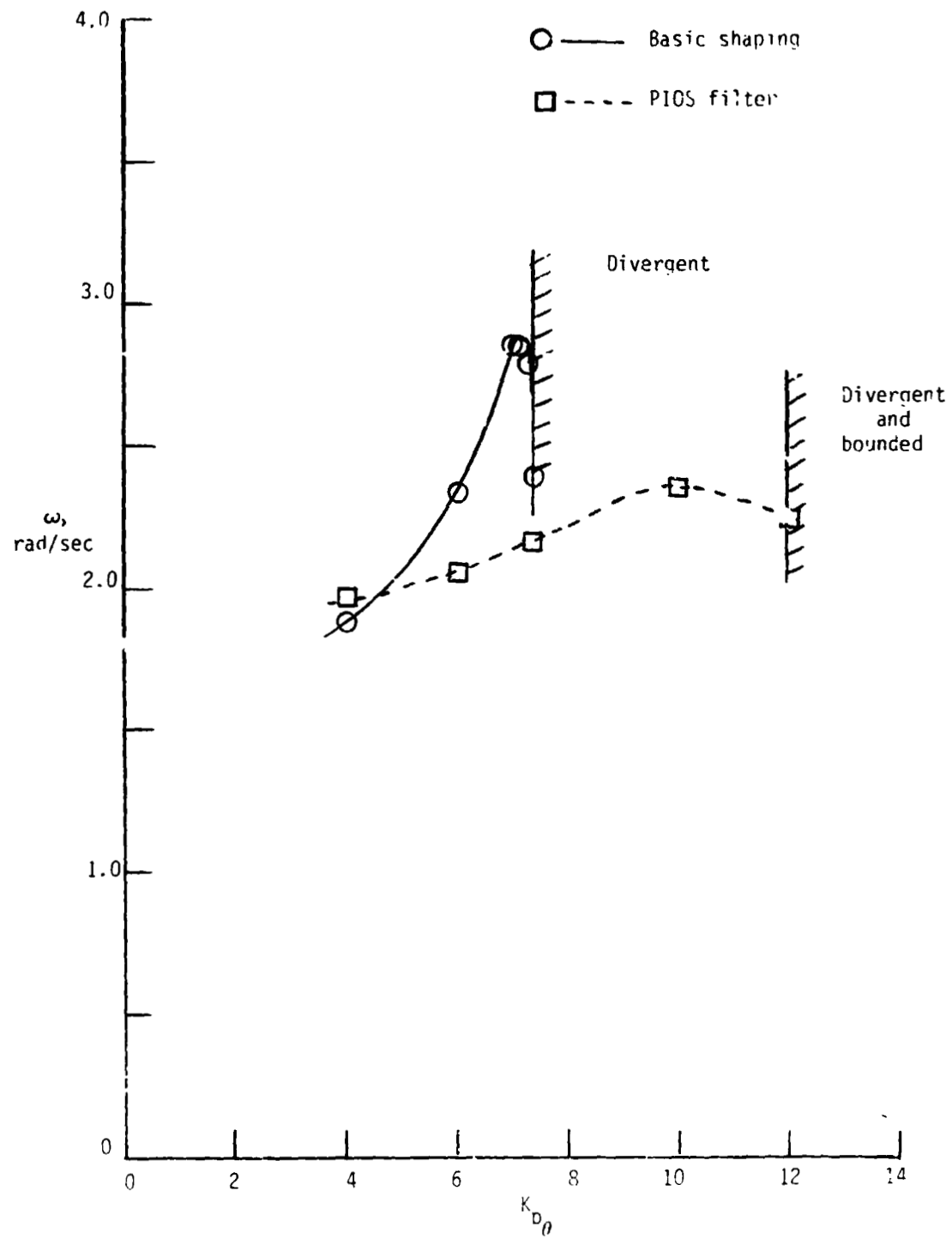


Figure 10. Shuttle simulation using a closed loop attitude system with pure gain for a pilot model, $K_{p_{\theta}} = 7.3$ (see fig. 1).



(a) Variation of subsidence ratio with pilot gain.

Figure 11. Shuttle simulation using a closed-loop attitude system with pure gain for a pilot model (fig. 1).



(b) Variation of frequency with pilot gain.

Figure 11. Concluded.

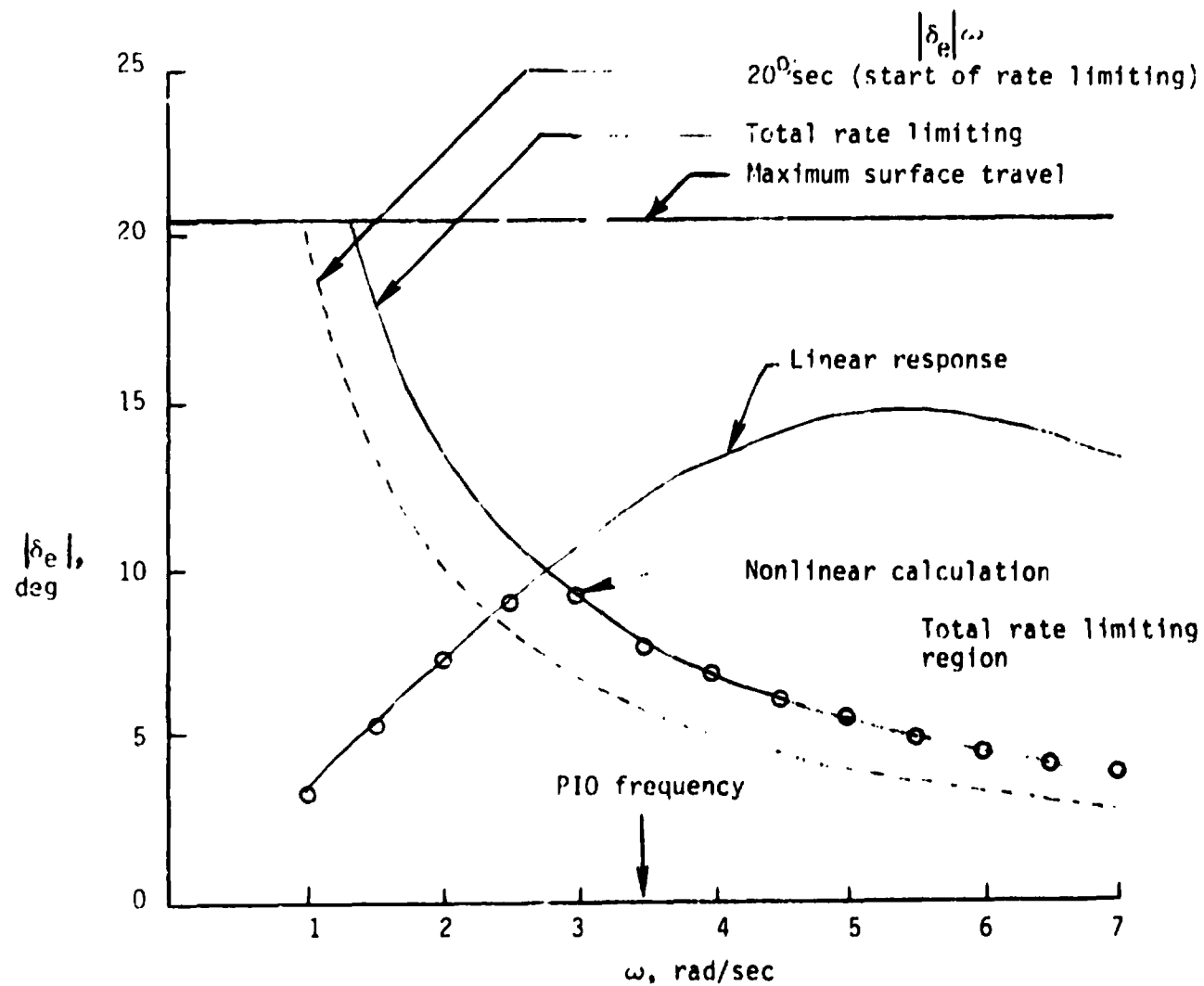


Figure 12. Elevator rate saturation boundaries and the predicted linear elevator response for the shuttle landing as a function of frequency for a pilot input, DEP, of 10 degrees.

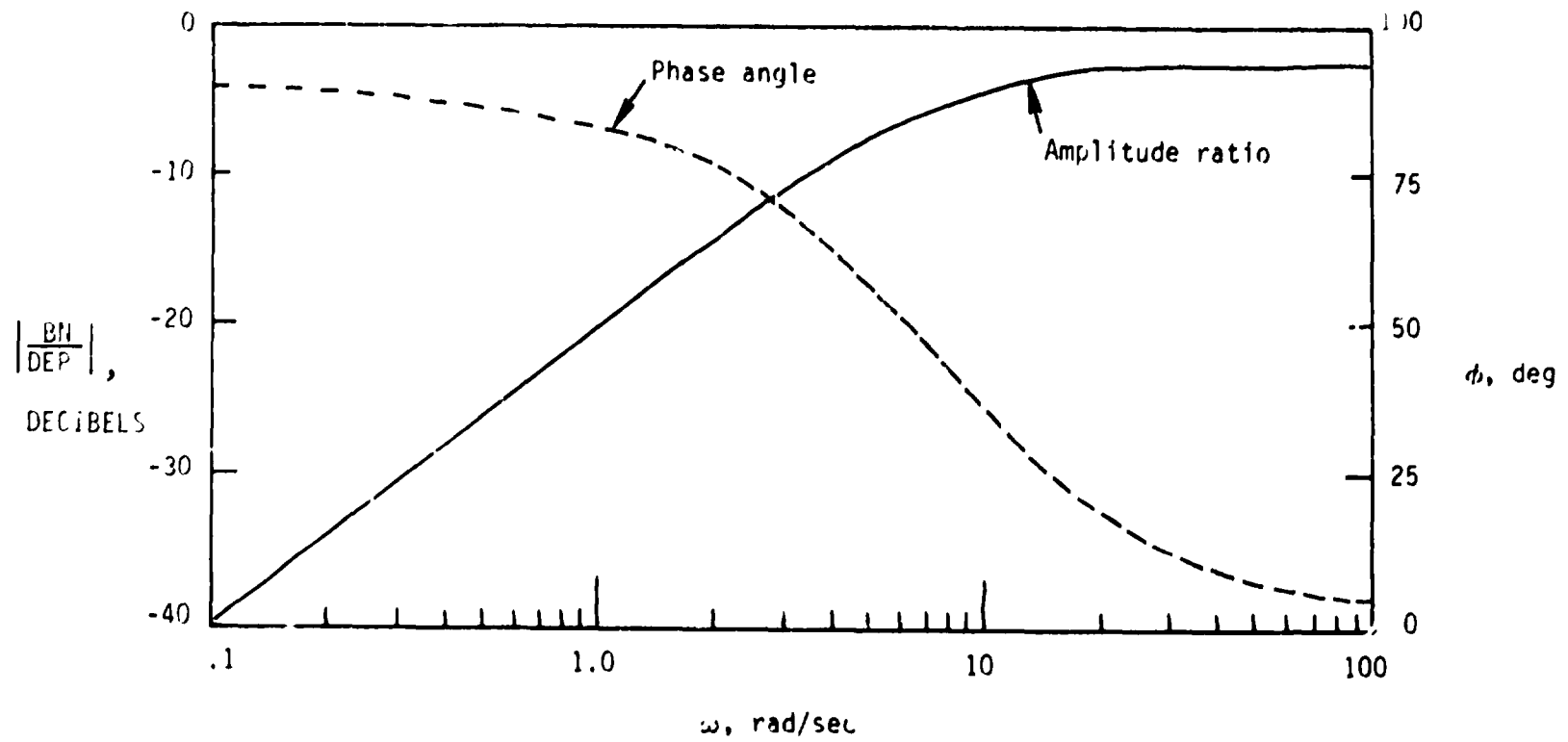


Figure 13. Amplitude ratio and phase angle, as a function of frequency,

$$\frac{BN}{DEP} = 1 - \frac{1}{4} \frac{(s + 20)^2}{(s + 10)^2}.$$

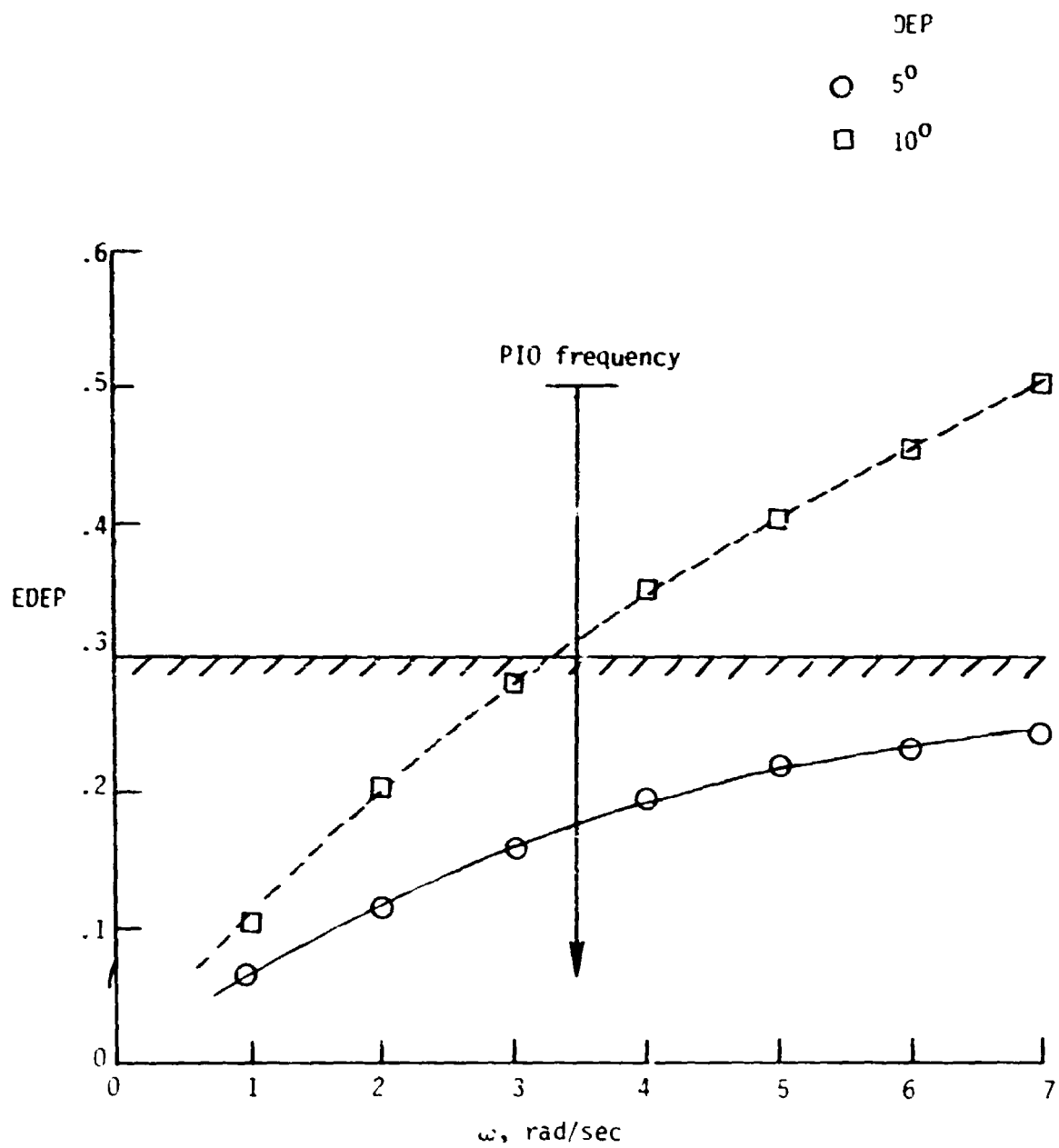


Figure 14. Steady state output ratio, EDEP, is a function of frequency and input amplitude.